SPANDIDOS PUBLICATIONS

ONCOLOGY LETTERS 11: 1007-1015, 2016

Genomic mapping of pathways in endometrial adenocarcinoma and a gastrointestinal stromal tumor located in Meckel's diverticulum

MONIKA ENGLERT-GOLON[1*], BARTLOMIEJ BUDNY[2*], BARTOSZ BURCHARDT[1], ELZBIETA WROTKOWSKA[2], KATARZYNA ZIEMNICKA[2], MAREK RUCHAŁA[2] and STEFAN SAJDAK[1]

[1]Surgical Gynecology Clinic of the Gynecological and Obstetrics Clinical Hospital; [2]Department of Endocrinology, Metabolism and Internal Diseases, Poznan University of Medical Sciences, 60-535 Poznan, Poland

Received November 16, 2014; Accepted October 13, 2015

DOI: 10.3892/ol.2015.4004

Abstract. The present study reports the case of a 71-year-old female patient diagnosed with endometrial adenocarcinoma, which was confirmed by histopathology. In the course of performing an elective hysterectomy with adnexa removal, a solid tumor located in Meckel's diverticulum (MD) was identified and excised. Due to the unique nature of the lesion, the tumor tissue underwent broad mapping of any genomic alterations once the histopathological examination was completed. The genetic testing was conducted using a high-resolution microarray and resulted in the identification of 45 genomic abnormalities, including 4 chromosomal aneuploidies. Within those regions, alterations of 87 known cancer genes were assigned. The involvement of v-kit Hardy-Zuckerman 4 feline sarcoma viral oncogene homolog gene alteration was noted to be a key player for triggering gastrointestinal stromal tumor transformation for this unusual case. A total of 12 genes, showing mutual interaction in different cancer types or involved in diverse cellular processes, were identified. These reported data may shed light on the carcinogenesis of a rare MD tumor.

Introduction

Gastrointestinal stromal tumors (GISTs) are the most frequent mesenchymomas of the gastrointestinal tract with a smooth muscle origin. The application of immunohistochemistry to the study of GISTs, provides novel insights into the disorder, revealing the contribution of the interstitial cells of Cajal, the spindle cells of the gut wall (1-4). The majority of GISTs are located within the stomach (50-70%) or the small intestine (20-30%), with as few as 10% of the tumors developing in the rectum, and only 5% developing in the large intestine, the retroperitoneal space and a variety of other locations (i.e., appendix and pancreas) (5,6). These tumors are even less frequent within the mesentery, omentum and esophagus (7).

The age of onset for GIST patients is broad, but the tumors commonly occur at 50-60 years. Precise GIST diagnostics became possible only after the 1998 discovery of the c-kit proto-oncogene and cluster of differentiation (CD)117 protein overexpression in the tumor cells (8). The biological nature of these tumors, indispensably link the activity of v-kit Hardy-Zuckerman 4 feline sarcoma viral oncogene homolog (KIT) kinase and platelet-derived growth factor receptor α (*PDGFRA*) in cancer progression (9-11). Notably, 10-15% of tumor cases are not associated with these genes (designated as *KIT*/*PDGFRA* wild-type), but rather to different carcinogenesis contributors, such as the succinate dehydrogenase complex and mutations of neurofibromin 1, B-Raf proto-oncogene, serine/threonine kinase or Kirsten rat sarcoma viral oncogene homolog kinase (12,13). This broad genetic heterogeneity of GIST highlights the complexity of the tumor origin, but more importantly, further affects the varied responsiveness of GISTs to treatment with the tyrosine kinase inhibitors (14).

Meckel's diverticulum (MD) is the most frequent congenital defect of the small intestine and is present in ~2% of the general population. Neoplasms of MD are diagnosed only in 0.5-3.2% of the population carrying this anatomical defect (15). To date, GISTs of MD origin have not been investigated thoroughly at the genomic level. However, a few case studies have described the tumor tissue examination, showing positive immunohistochemistry reactions for vimentin and c-kit, therefore indicating the GIST nature (15-17). A previous epidemiological study on 163 MD cases has indicated that MD is a cancer 'hot-spot', comprising an attractive location for tumor development (18). Moreover, when comparing different types of cancer, an apparent preponderance of adenocarcinomas versus malignant carcinoids (2:1 ratio) was observed.

Correspondence to: Professor Stefan Sajdak, Surgical Gynecology Clinic of the Gynecological and Obstetrics Clinical Hospital, Poznan University of Medical Sciences, Polna 33, 60-535 Poznan, Poland
E-mail: kgo.ela@wp.pl

*Contributed equally

Key words: endometrial adenocarcinoma, gastrointestinal stromal tumor, Meckel's diverticulum, microarrays, *KIT* gene

The present study attempted to comprehensively explore and reveal the genetic nature of the rare cancer tissue located in MD and investigate its GIST origin.

Patients and methods

Patient. A 71-year-old woman reported to the Obstetrics and Gynecology Emergency Room (Clinical Hospital, Poznan, Poland) on December 3, 2011, due to newly occurring postmenopausal bleeding. A biopsy of the endometrium was performed and the material obtained was assessed by the Pathology Laboratory. The results of the histopathological examination indicated endometrioid adenocarcinoma (G1). Following the diagnosis, the patient was admitted to the hospital for further treatment. Subsequent to being admitted to the Surgical Gynecology Clinic of the Gynecological and Obstetrics Clinical Hospital, the patient underwent a gynecological examination and a transvaginal ultrasound. Following a cardiology consultation, the patient qualified for elective surgical treatment. During the surgery, the entire uterus with adnexa was removed, and a solid tumor of ~3 cm in size, which was previously not visible in the ultrasound image, was found in MD. The procedure included a complete resection of the tumor along with the diverticulum and an end to end intestinal anastomosis. Tissue samples were sent for a histopathological examination. No intraoperative examinations were performed. There were no complications in the post-operative period or during recovery following the intestinal anastomosis. The patient was discharged from the hospital on the 7th day after the surgery in a good general condition. The patient was advised to await the histopathological examination results and was informed that a decision concerning any further course of treatment would be made based on these results.

Genetic examination. Once the treatment was completed, advanced molecular testing was employed in order to identify tumor-specific genome changes. Briefly, the Genome-Wide Human CytoScan HD Array and CytoScan 750K (Affymetrix, Santa Clara, CA, USA) was used to analyze genomic alterations in the tumor sample. Genomic DNA was obtained from formalin-fixed paraffin-embedded (FFPE) sections using conventional processing (deparaffinization, enzymatic treatment and DNA extraction) (19). The 250 ng of genomic DNA from the tumor was subjected to microarray examination according to the manufacturer's protocols as follows: i) Digestion with the restriction enzyme *Nsp*I; ii) adapter ligation, polymerase chain reaction (PCR) amplification and magnetic bead purification; iii) fragmentation and end-labeling with biotin; iv) washing and staining using a GeneChip® Fluidics Station 450; and v) scanning using an Affymetrix GeneChip Scanner 3000 7G (Affymetrix). Scanned data files were generated using Affymetrix GeneChip Command Console Software, version 1.2, and analyzed with Affymetrix Chromosome Analysis Suite v 2.0.0.195 (Affymetrix). To calculate the copy number of altered regions, the data were normalized to baseline reference intensities using NA 32.3 FFPE v.2 reference model (Affymetrix). The hidden Markov model available within the software package was used to determine the copy number states (CN) and their breakpoints. Thresholds of $\log_2$ ratio ≥0.58 and ≤1 were used to categorize altered regions as CN variation (CNV) gains (amplifications) and copy number losses (deletions), respectively. To prevent the detection of false-positive CNVs arising due to microarray unspecific signals, only regions that involved at least 50 consecutive probes were considered in the analysis of gains or losses in this study. Amplifications and deletions were analyzed separately. To exclude aberrations representing common normal CNVs, all the identified CNVs were compared with those reported in the Database of Genomic Variants (http://projects.tcag.ca/variation/). To identify the genes involved in the CNVs further, the UCSC database (http://genome.ucsc.edu) and Ensemble (http://www.ensembl.org) were used. Gene annotation and gene overlap were determined using the human genome build 19 and NetAffx (http://www.affymetrix.com). In addition, the identified alterations were compared with COSMIC database (http://cancer.sanger.ac.uk) (20) to look for overlap with up-to-date, known genomic cancer regions and single cancer genes. The algorithm for the detection of copy number aberrations in tumor cell mixtures (mosaicism and clonality) considers the comprehensive analysis of adjacent single copy deletions and gains segments. The algorithm is designed to be most accurate when the normal/expected CN is diploid and targets the detection of changes in regions of ~5 Mb or more in size and variation with a minimum of 500 markers (being typical for segments of 5,000 markers or more). This approach considers only a discrete number of mosaicism levels, which are set at 30, 50 and 70%. The range of log ratios is broken into a series of bands according to the detection level (≥30, ≥50% or 70-100% bands) and log ratios within each band denote a specific copy number change event. This tool is most efficient in detecting mosaicism between 30-70% of cells and for copy numbers between 1 and 3. Selected regions were validated in the present study using quantitative PCR ($2^{-\Delta\Delta Cq}$; *KIT* gene).

Results

Clinical findings. The results of the histopathological examination indicated endometrioid adenocarcinoma (G1) and a uterine leiomyoma; GIST, T2 (immunophenotype: CD117$^+$, CD34$^+$ and vimentin$^+$). Laboratory tests, a gynecological examination and transvaginal ultrasound were performed during the next hospital stay. No indications for chemotherapy were identified, the radical nature of the surgery was confirmed, as well as the complete removal of the lesion. After a single day of in-patient treatment, the patient was discharged in a good general condition and was recommended to undergo whole-body positron emission tomography-computed tomography. The scan was performed 12 months after the last hospitalization. No pathological tracer uptake areas were identified. At present, the patient is under the care of the Oncology Outpatient Clinic. No episodes of recurrence had been identified at the time of preparing the manuscript for this case study.

Genomic studies. The strategy for the reliable detection of chromosomal rearrangements assumes usage of the CytoScan 750K chip in the first step. This investigation resulted in detection of ~62 genomic imbalances that were not filtered out and passed the genomic criteria (>400 kb; 50 markers). To confirm abnormalities and fine mapping of the borders for genomic segments, a high-resolution chip Cytoscan HD (2.7 million probes and high coverage of 522 cancer genes) was applied. The

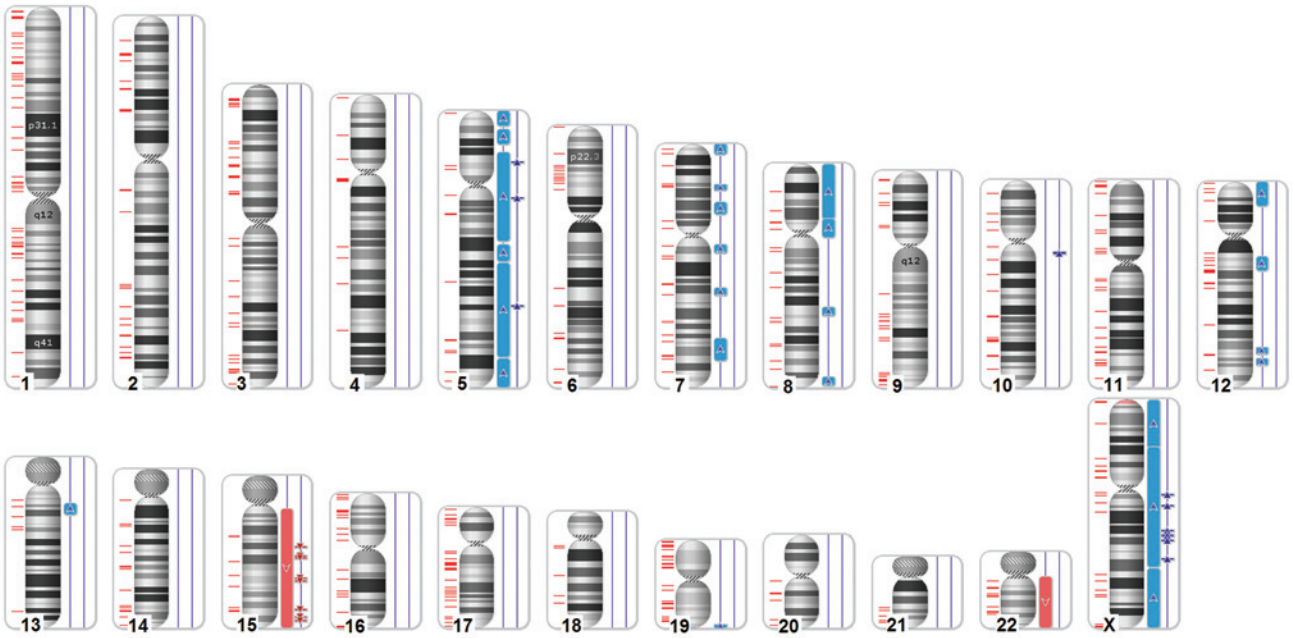

Figure 1. A karyoview of identified genomic abnormalities (right of each ideogram). Gains are shown in blue bars (regions of CN2-3 in light blue and CN≥3 in dark blue). Losses are shown analogically in red bars (regions of CN1-2 in light red and CN≤1 in dark red). The location and distribution of 522 cancer genes (COSMIC) are indicated on the left of ideogram. CN, copy number states.

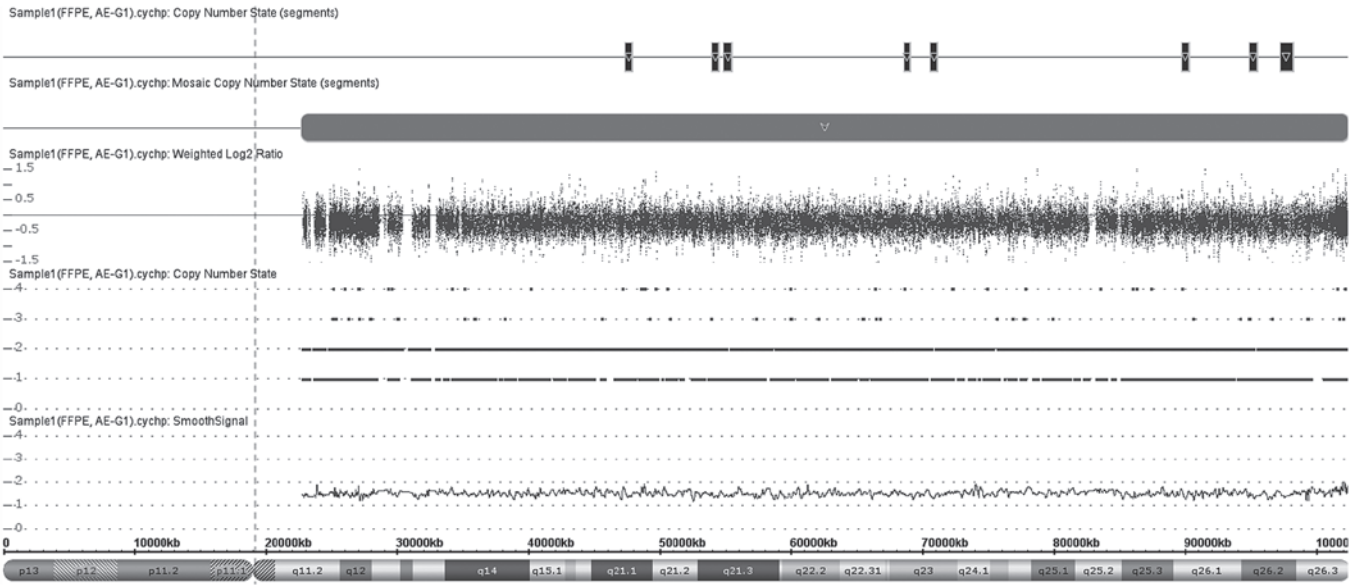

Figure 2. An example of microarray analysis of chromosome 15. Log_2 ratio and copy number state in examined formalin-fixed paraffin-embedded (FFPE) tumor tissue are shown.

unbiased density of probes on the chip enabled improvements to the accuracy and confidence of detected regions. A total of 45 previously detected regions were confirmed, and 17 other segments were disregarded as false-positives (signal noise, more rigorous filtering criteria compared with CytoScan 750K chip and usage of FFPE reference model for Cytoscan HD that is far more accurate). In total, the cancer tissue revealed alterations on 6 chromosomes (chromosomes 7, 8, 10, 12, 13 and 19) and 4 entire chromosome aneuploidies (chromosomes 5, 15, 22 and X). A dedicated karyogram illustrating the localization of each segment is shown in Fig. 1, and an example of mosaic aneuploidy (chromosome 15) is shown in Fig. 2. The genomic regions where than divided into 4 groups: Low mosaic gains (CN2-3), low mosaic losses (CN2-1), amplifications (CN>3) and deletions suggestive for loss of heterozygosity (CN<1). All these data and precise genomic coordinates were incorporated into Table I. Within detected intervals, 4,803 genes were identified. Having high microarray reproducibility, less rigorous criteria were applied to narrow down the abnormality size up to 100 kb (with 50 markers unchanged) to evaluate smaller rearrangements, expanding the genomic area to 442 segments. A focus was placed particularly on known cancer genes (522 entities) and

Table I. Genomic alterations (>400 kb in size) found in examined tumor. Any overlapping cancer genes (COSMIC) are additionally listed using gene ID.

Case	CN	Type	Chromosome	Cytoband start	Start	End	Size, kbp	Gene count, total	Census gene count	Gene name (s)
1	2.29	Gain	5	p15.33	113576	10070760	9957.184	63	1	TERT
2	2.25	Gain	5	p15.2	12452650	21850508	9397.858	19		
3	2.33	Gain	5	p14.1	27490784	85587655	58096.871	274	4	IL7R, IL6ST, PIK3R1, LIFR
4	>3	Gain	5	p13.3	33484586	33897522	412.936	1		
5	>3	Gain	5	q11.2	56710608	57133644	423.036	1		
6	2.25	Gain	5	q14.3	87860680	98769659	10908.979	42		
7	2.33	Gain	5	q21.1	99756189	160909509	61153.32	438	5	CD74, ITK, EBF1, APC, PDGFRB
8	>3	Gain	5	q23.3	127572667	128144311	571.644	1		
9	2.32	Gain	5	q34	161866188	180719789	18853.601	159	4	NPM1, RANBP17, NSD1, TLX3
10	2.23	Gain	7	p22.3	43360	6483365	6440.005	75	3	PMS2, CARD11, RAC1
11	2.21	Gain	7	p15.2	26483627	30210591	3726.964	42	4	HOXA11, HOXA9, HOXA13, JAZF1
12	2.29	Gain	7	p14.1	37893184	45800150	7906.966	70		
13	2.22	Gain	7	q11.21	66150834	71291670	5140.836	14		SBDS
14	2.22	Gain	7	q21.3	94402911	98900790	4497.879	32	1	TRRAP
15	2.25	Gain	7	q31.33	126728205	141381467	14653	127	4	KIAA1549, CREB3L2, SMO, BRAF
16	2.22	Gain	8	p23.3	158048	35996434	35838.386	255		PCM1, WRN
17	2.24	Gain	8	p12	36003284	48320037	12316.753	66	3	HOOK3, FGFR1, WHSC1L1
18	2.22	Gain	8	q22.1	93943335	99747954	5804.619	46		
19	2.22	Gain	8	q24.23	139395919	145287179	5891.26	77		
20	>3	Gain	10	q11.22	46976673	48174779	1198.106	17		
21	2.26	Gain	12	p13.33	173786	15842149	15668.363	244	4	ZNF384, KDM5A, CCND2, ETV6,
22	2.22	Gain	12	q13.11	49073505	57666097	8592.592	253	5	HOXC11, KMT2D, HOXC13, NACA, ATF1
23	2.22	Gain	12	q23.3	107607681	112259343	4651.662	58	2	SH2B3, ALDH2,
24	2.22	Gain	12	q24.21	114772266	119550739	4778.473	23		
25	2.24	Gain	13	q12.3	31303510	38510652	7207.142	43	1	BRCA2
26	1.47	Loss	15	q11.2	22770421	102429112	79658.691	799	8	BLM, PML, NTRK3, TCF12, IDH2, CRTC3, BUB1B, MAP2K1
27	<1	Loss	15	q21.1	47407284	47903647	496.363	1		
28	<1	Loss	15	q21.3	53994492	54476263	481.771	2		
29	<1	Loss	15	q21.3	54866217	55494071	627.854	2		
30	<1	Loss	15	q23	68667321	69080873	413.552	3		
31	<1	Loss	15	q23	70688921	71128704	439.783	2		
32	<1	Loss	15	q26.1	89819011	90281381	462.37	11		
33	<1	Loss	15	q26.2	94991252	95497814	506.562	1		
34	<1	Loss	15	q26.2	97288627	98205766	917.139	1		
35	2.25	Gain	19	q13.43	56862882	58956888	2094.006	75		

Table I. Continued.

Case	CN	Type	Chromosome	Cytoband start	Start	End	Size, kbp	Gene count, total	Census gene count	% of overlap map item covered by segment
36	1.7	Loss	22	q11.1	16888899	50902452	34013.553	525	11	CHEK2, MKL1, CLTCL1, NF2, EWSR1, MN1, SMARCB1, PDGFB, EP300, MYH9, BCR
37	2.32	Gain	X	p22.33	168546	32908751	32740.205	165	3	CRLF2, ZRSR2, P2RY8,
38	2.46	Gain	X	p21.1	32388483	113724212	81335.729	488	14	SSX1, MSN, KDM5C, KDM6A, ATRX, BCOR, SSX2, NONO, GATA1, TFE3, SSX4, AMER1, WAS, MED12
39	>3	Gain	X	q11.2	64280772	64692636	411.864	0		
40	>3	Gain	X	q13.2	71859817	72307913	448.096	8		
41	>3	Gain	X	q21.31	88759463	89169371	409.908	0		
42	>3	Gain	X	q21.32	91923926	92392650	468.724	0		
43	>3	Gain	X	q21.33	95094694	95611952	517.258	1		
44	>3	Gain	X	q22.3	108029759	108614975	585.216	0		
45	2.38	Gain	X	q23	114896478	155233731	40337.253	345	8	ATP2B3, PHF6, STAG2, SEPT6, GPC3, RPL10, ELF4, MTCP1

CN, copy number state.

Table II. COSMIC database reporting genes to be mutated in gastrointestinal tract (site indeterminate and various tumor types) and small intestine adenocarcinoma.[a]

Case	Gene	Mutated samples	Sample tested
1	*NRAS*	79	502
2	*HRAS*	31	495
3	***TERT***	**28**	**97**
4	*KRAS*	19	490
5	*PIK3CA*	14	194
6	*PTEN*	11	150
7	***BRAF***	**8**	**595**
8	*TSHR*	8	50
9	*IDH1*	6	53
10	*CDKN2A*	4	28
11	*MET*	2	41
12	*TP53*	2	20
13	*GNAS*	2	73
14	*PAX8*	0	142
15	*EGFR*	0	101
16	*CCDC6*	0	80
17	*PDGFRA*	0	64
18	***KIT***	**0**	**64**
19	*NCOA*	0	55
20	*GNA11*	0	46
21	*GNAQ*	0	42
22	***PIK3R1***	**0**	**34**
23	***IDH2***	**0**	**32**
24	*AKT1*	0	23
25	*ALK*	0	22
26	*RET*	0	21
27	*PRKAR1A*	0	16
28	*MEN1*	0	15
29	***APC***	**0**	**15**
30	***MAP2K1***	**0**	**13**
31	*STRN*	0	11
32	*VHL*	0	10
33	***NPM1***	**0**	**10**
34	*CDH1*	0	8
35	*TFG*	0	6
36	*TPR*	0	6
37	*JAK2*	0	6
38	*CTNNB1*	0	4
39	*SF3B1*	0	4
40	***KDM6A***	**0**	**4**
41	*SMAD4*	0	4
42	*PTPN11*	0	3
43	*TPM3*	0	2

[a]Genes contributing to the case and found within altered regions are in bold.

associated pathways that contribute to adenocarcinoma in MD. In order to divulge putative genes contributing to MD adenocarcinoma, the regions for COSMIC genes (known also as Census

Table III. Kyoto Encyclopedia of Genes and Genomes pathway and statistical analysis for involvement of selected cancer genes present in altered genomic regions and their contribution to different cancer types or cellular control.

Case	Gene ontology ID	Term	P-value	No. of genes	Genes
1	hsa05200	Pathways in cancer	$1.29x10^{-6}$	12	*BCR*, *APC*, *SMO*, *PDGFRB*, *PDGFB*, *EP300*, *BRAF*, *MAP2K1*, *PIK3R1*, *BRCA2*, *FGFR1*, *PML*
2	hsa05215	Prostate cancer	$1.27x10^{-7}$	8	*CREB3L2*, *PIK3R1*, *PDGFRB*, *PDGFB*, *EP300*, *FGFR1*, *BRAF*, *MAP2K1*
3	hsa05218	Melanoma	$7.8x10^{-6}$	6	*PIK3R1*, *PDGFRB*, *PDGFB*, *FGFR1*, *BRAF*, *MAP2K1*
4	hsa05214	Glioma	$6.4x10^{-5}$	5	*PIK3R1*, *PDGFRB*, *PDGFB*, *BRAF*, *MAP2K1*
5	hsa04630	Jak-STAT signaling pathway	$8.73x10^{-5}$	7	*PIK3R1*, *IL7R*, *CCND2*, *CRLF2*, *IL6ST*, *EP300*, *LIFR*
6	hsa05211	Renal cell carcinoma	$1.08x10^{-4}$	5	*PIK3R1*, *PDGFB*, *EP300*, *BRAF*, *MAP2K1*
7	hsa05213	Endometrial cancer	$4.39x10^{-4}$	4	*APC*, *PIK3R1*, *BRAF*, *MAP2K1*
8	hsa05221	Acute myeloid leukemia	$5.87x10^{-4}$	4	*PIK3R*, *PML*, *BRAF*, *MAP2K1*
9	hsa05210	Colorectal cancer	$6.73x10^{-4}$	4	*APC*, *PIK3R1*, *BRAF*, *MAP2K1*
10	hsa05212	Pancreatic cancer	$1.04x10^{-3}$	4	*PIK3R1*, *BRCA2*, *BRAF*, *MAP2K1*
11	hsa05220	Chronic myeloid leukemia	$1.38x10^{-3}$	4	PIK3R1, *BRAF*, *MAP2K1*, *BCR*
12	hsa04110	Cell cycle	$1.51x10^{-3}$	5	*CCND2*, *CHEK2*, *STAG2*, *EP300*, *BUB1B*
13	hsa04510	Focal adhesion	$2.43x10^{-3}$	6	*PDGFRB*, *PDGFB*, *BRAF*, *MAP2K1*, *PIK3R1*, *CCND2*
14	hsa05223	Non-small cell lung cancer	$5.86x10^{-3}$	3	*PIK3R1*, *BRAF*, *MAP2K1*
15	hsa04062	Chemokine signaling pathway	$8.99x10^{-3}$	5	*PIK3R1*, *WAS*, *BRAF*, *MAP2K1*, *ITK*
16	hsa04060	Cytokine-cytokine receptor interaction	$9.63x10^{-3}$	6	*CRLF2*, *IL6ST*, *PDGFRB*, *PDGFB*, *LIFR*, *IL7R*

JAK/STAT, Janus kinase/signal transducer and activator of transcription.

Genes) (21-23) were assessed and 88 entities were selected, 43 of which were recurrent (Table II). In order to further delineate the putative cancer pathways, gene-interactions were searched for using the Kyoto Encyclopedia of Genes and Genomes (KEGG) pathway database (http://www.genome.jp/kegg) (24). In total, 16 KEGG pathways were selected that are associated with the development of different types of cancer or cellular regulation processes (Table III). Interacting genes were visualized as a network using String version 9.1 (http://string-db.org) (Fig. 3) (25).

Discussion

Current studies are aimed at estimating the incidence of GIST cases in the population. Swedish studies have shown that currently, the number of novel GIST cases amounts to 15-16 million/year (26). A tumor may develop in any section of the gastrointestinal tract, as well as intraperitoneally and in the retroperitoneal space. The current state of knowledge and statistical data indicate that when a radical surgical excision of the tumor is possible, the 5-year survival rate is 50-60% (27,28). At the same time, literature references indicate that 80% of patients who undergo surgery experience local recurrence within 2 years of the procedure, and that liver metastases additionally appear in 50% of the patients (29,30). In the case discussed in the present study, the patient was treated surgically for reasons other than a GIST. This problem is widely discussed in the literature. Approximately 40% of women with small intestine GISTs undergo surgery due to genital tract tumors (GIST mimicking pelvic disorders). The genetic mapping of major molecular contributors, tyrosine kinases *KIT* and *PDGFRA* (ref. NM_000222 and NM_006206), reveal that they are located very close to each other on chromosome 4 (31,32) and are found to be mutated in up to 90% of GIST cases. For each, a gain of function mutations results in constitutive activation of the oncogenes, but the clinical consequences may differ significantly (33,34). The biological consequences related to abnormal hyperactivity of both proteins observed in cancer cells for each gene implies the occurrence of a variety of possible mechanisms,

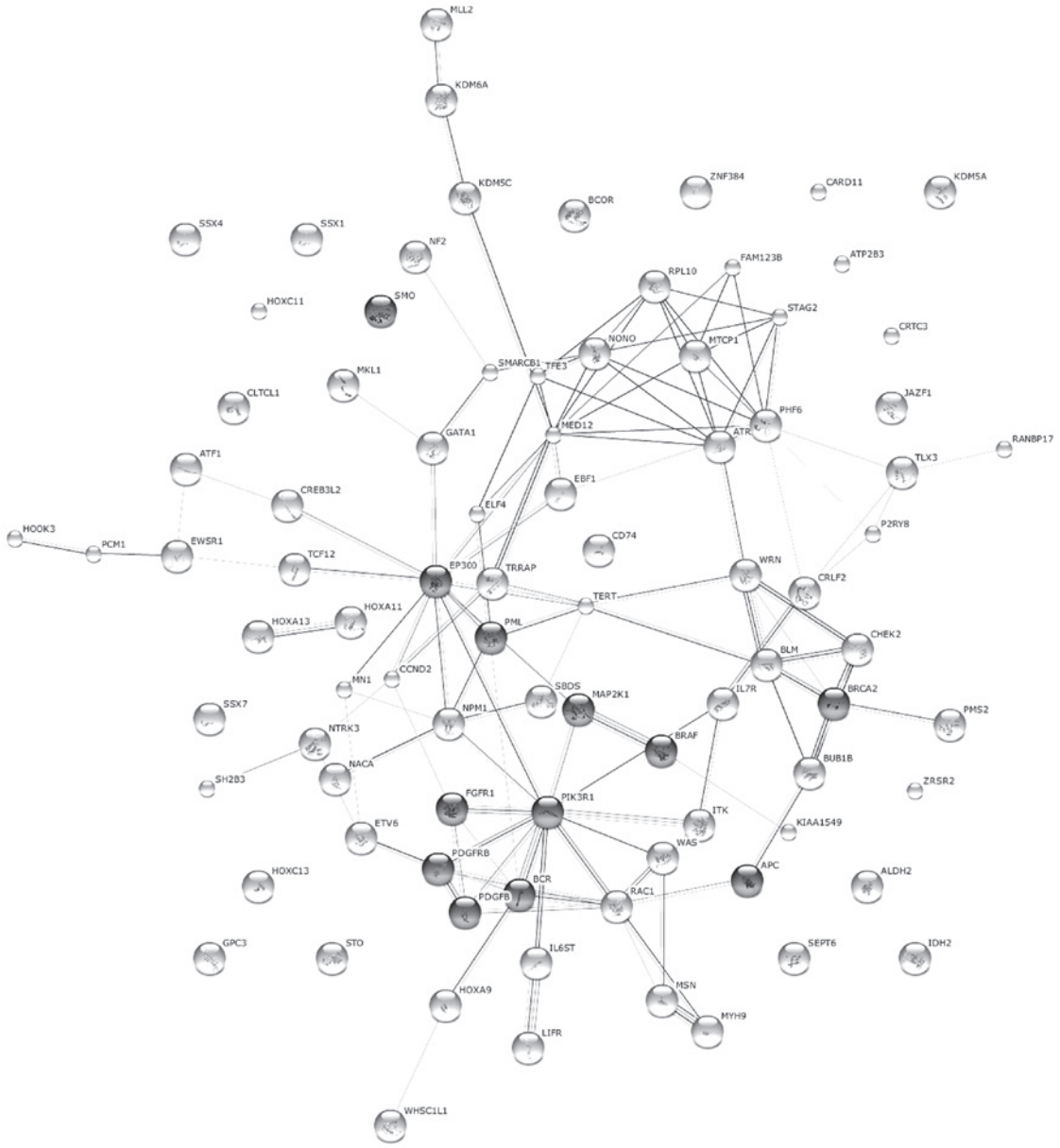

Figure 3. String visualization of the network interaction of all 87 selected cancer proteins. Proteins reported to be altered and contributing to Kyoto Encyclopedia of Genes and Genomes 'Pathways in cancer' (hsa05200; Table III) are indicated in dark gray (12 genes).

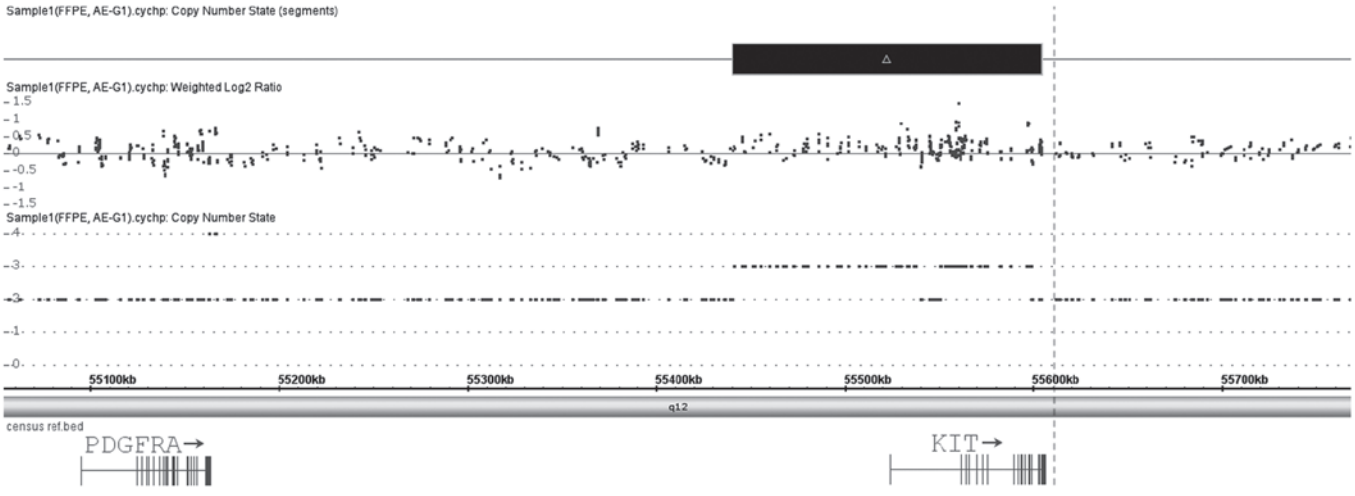

Figure 4. A high-resolution examination of 4q12 region presenting amplification of the *KIT* gene and no copy number state alteration of the *PDGFRA* gene. *PDGFRA*, platelet-derived growth factor receptor α; FFPE, formalin-fixed paraffin-embedded.

including point mutations and bigger genomic instabilities (whole gene amplifications or gene fusions). Hence, the comprehensive molecular portrait of GIST cancers is now emerging. This is possibly due to usage of high-throughput genomic approaches that provide valuable data referring to the involvement of a single gene, but also characterizing entire pathways on various stages of GIST carcinogenesis (35-37). To date, high-resolution mapping has been conducted only by two groups (36,38), with reference to typical GIST occurrences. Specific chromosomal rearrangements are solid and a consistent finding accompanying KIT and PDGFRA alterations. Losses of chromosomes 1, 3, 13, 14, 15 and 22, whereas gains of chromosomes 4 and 5 may represent clinical utility and prognostic relevance. In the present case, a 15q loss was identified, which is regarded as an aggressive course for a GIST. The loss of 1p was also noted, which is typical for the small intestine localization of tumors, and the absence of a copy number alteration in the *RB1* locus, which is known as a strong clinical predictor (39). Application of a high-resolution microarray allows the identification of CN changes at a single gene level (for constitutional disorders, even single exon rearrangements). In the present study, *KIT* gene amplification was detected on chromosome 4, spanning only 163 kb and comprising the entire genomic sequence of this gene. Unexpectedly, the closely located PDGFRA gene (400 kb away) was not altered (Fig. 4). This finding is reminiscent and indicative of the principal role of KIT in triggering oncogenesis in this case. However, an activating point mutation in another gene cannot be excluded. Alteration of two prominent interacting proteins, PDGFRB and PIK3R1 (40), was also found. Phosphorylation of phosphatidylinositol 3-kinase (PIK3R1) by KIT leads to the activation of the v-akt murine thymoma viral oncogene homolog 1 signaling pathway. Activated KIT also transmits signals via growth factor receptor-bound protein 2 and activation of RAS, Raf-1 proto-oncogene, serine/threonine kinase and the mitogen-activated protein kinases (MAPKs) MAPK1/ERK2 and/or MAPK3/ERK1.

In conclusion, by employing a high-resolution microarray, the present study performed a comprehensive genomic analysis on genes contributing to GISTs, in the rare location of MD. A principal role of the *KIT* gene was confirmed in cancer initiation, which was demonstrated by detailed histopathological and molecular investigations. The detected chromosomal gains and losses were consistent with the findings of a GIST and confirm previous studies. Possible chemokine and cytokine-related signaling pathways (PIK3R1, BRAF, MAP2K1, PDGFRB and PDGFB) that may reasonably contribute to cancer progression with GIST characteristics were also indicated.

Acknowledgements

This study was supported by the grant no. 789/FNiTP/162/2013 Polish Ministry of Science and Education.

References

1. Sircar K, Hewlett BR, Huizinga JD, Chorneyko K, Berezin I and Riddell RH: Interstitial cells of Cajal as precursors of gastrointestinal stromal tumors. Am J Surg Pathol 23: 377-389, 1999.
2. Chan JK: Mesenchymal tumors of the gastrointestinal tract: A paradise for acronyms (STUMP, GIST, GANT, and now GIPACT), implication of c-kit in genesis, and yet another of the many emerging roles of the interstitial cell of Cajal in the pathogenesis of gastrointestinal diseases? Adv Anat Pathol 6: 19-40, 1999.
3. Rutkowski P, Debiec-Rychter M and Ruka W: Gastrointestinal stromal tumors: Key to diagnosis and choice of therapy. Mol Diagn Ther 12: 131-143, 2008.
4. Rutkowski P, Wozniak A, Dębiec-Rychter M, Kąkol M, Dziewirski W, Zdzienicki M, Ptaszynski K, Jurkowska M, Limon J and Siedlecki JA: Clinical utility of the new American Joint Committee on Cancer staging system for gastrointestinal stromal tumors: Current overall survival after primary tumor resection. Cancer 117: 4916-4924, 2011.
5. Corless CL, Fletcher JA and Heinrich MC: Biology of gastrointestinal stromal tumors. J Clin Oncol 22: 3813-3825, 2004.
6. Miettinen M, Sarlomo-Rikala M and Lasota J: Gastrointestinal stromal tumors: Recent advances in understanding of their biology. Hum Pathol 30: 1213-1220, 1999.
7. Roberts PJ and Eisenberg B: Clinical presentation of gastrointestinal stromal tumors and treatment of operable disease. Eur J Cancer 38 (Suppl 5): S37-S38, 2002.
8. Neuhaus SJ, Clark MA, Hayes AJ, Thomas JM and Judson I: Surgery for gastrointestinal stromal tumour in the post-imatinib era. ANZ J Surg 75: 165-172, 2005.
9. Duensing A, Heinrich MC, Fletcher CD and Fletcher JA: Biology of gastrointestinal stromal tumors: KIT mutations and beyond. Cancer Invest 22: 106-116, 2004.
10. Heinrich MC, Rubin BP, Longley BJ and Fletcher JA: Biology and genetic aspects of gastrointestinal stromal tumors: KIT activation and cytogenetic alterations. Hum Pathol 33: 484-495, 2002.
11. Huizinga JD, Thuneberg L, Klüppel M, Malysz J, Mikkelsen HB and Bernstein A: W/kit gene required for interstitial cells of Cajal and for intestinal pacemaker activity. Nature 373: 347-349, 1995.
12. Nannini M, Astolfi A, Urbini M, Indio V, Santini D, Heinrich MC, Corless CL, Ceccarelli C, Saponara M, Mandrioli A, *et al*: Integrated genomic study of quadruple-WT GIST (KIT/PDGFRA/SDH/RAS pathway wild-type GIST). BMC Cancer 14: 685, 2014.
13. Pantaleo MA, Nannini M, Corless CL and Heinrich MC: Quadruple wild-type (WT) GIST: Defining the subset of GIST that lacks abnormalities of KIT, PDGFRA, SDH, or RAS signaling pathways. Cancer Med 4: 101-103, 2014.
14. Heinrich MC, Griffith DJ, Druker BJ, Wait CL, Ott KA and Zigler AJ: Inhibition of c-kit receptor tyrosine kinase activity by STI 571, a selective tyrosine kinase inhibitor. Blood 96: 925-932, 2000.
15. Chandramohan K, Agarwal M, Gurjar G, Gatti RC, Patel MH, Trivedi P and Kothari KC: Gastrointestinal stromal tumour in Meckel's diverticulum. World J Surg Oncol 5: 50, 2007.
16. Khoury MG 2nd and Aulicino MR: Gastrointestinal stromal tumor (GIST) presenting in a Meckel's diverticulum. Abdom Imaging 32: 78-80, 2007.
17. Kosmidis C, Efthimiadis C, Levva S, Anthimidis G, Baka S, Grigoriou M, Tzeveleki I, Masmanidou M, Zaramboukas T and Basdanis G: Synchronous colorectal adenocarcinoma and gastrointestinal stromal tumor in Meckel's diverticulum; an unusual association. World J Surg Oncol 7: 33, 2009.
18. Thirunavukarasu P, Sathaiah M, Sukumar S, Bartels CJ, Zeh H III, Lee KK and Bartlett DL: Meckel's diverticulum - a high-risk region for malignancy in the ileum. Insights from a population-based epidemiological study and implications in surgical management. Ann Surg 253: 223-230, 2011.
19. Gillio-Tos A, De Marco L, Fiano V, Garcia-Bragado F, Dikshit R, Boffetta P and Merletti F: Efficient DNA extraction from 25-year-old paraffin-embedded tissues: Study of 365 samples. Pathology 39: 345-348, 2007.
20. Forbes SA, Bindal N, Bamford S, Cole C, Kok CY, Beare D, Jia M, Shepherd R, Leung K, Menzies A, *et al*: COSMIC: Mining complete cancer genomes in the Catalogue of Somatic Mutations in Cancer. Nucleic Acids Res 39 (Database): D945-D950, 2011.
21. Futreal PA, Coin L, Marshall M, Down T, Hubbard T, Wooster R, Rahman N and Stratton MR: A census of human cancer genes. Nat Rev Cancer 4: 177-183, 2004.
22. Pérez de Castro I, de Cárcer G and Malumbres M: A census of mitotic cancer genes: New insights into tumor cell biology and cancer therapy. Carcinogenesis 28: 899-912, 2007.
23. Santarius T, Shipley J, Brewer D, Stratton MR and Cooper CS: A census of amplified and overexpressed human cancer genes. Nat Rev Cancer 10: 59-64, 2010.

24. Altermann E and Klaenhammer TR: PathwayVoyager: Pathway mapping using the Kyoto Encyclopedia of Genes and Genomes (KEGG) database. BMC Genomics 6: 60, 2005.
25. Franceschini A, Szklarczyk D, Frankild S, Kuhn M, Simonovic M, Roth A, Lin J, Minguez P, Bork P, von Mering C, *et al*: STRING v9.1: Protein-protein interaction networks, with increased coverage and integration. Nucleic Acids Res 41 (D1): D808-D815, 2013.
26. Nilsson B, Bümming P, Meis-Kindblom JM, Odén A, Dortok A, Gustavsson B, Sablinska K and Kindblom LG: Gastrointestinal stromal tumors: The incidence, prevalence, clinical course, and prognostication in the preimatinib mesylate era - a population-based study in western Sweden. Cancer 103: 821-829, 2005.
27. Dematteo RP, Heinrich MC, El-Rifai WM and Demetri G: Clinical management of gastrointestinal stromal tumors: Before and after STI-571. Hum Pathol 33: 466-477, 2002.
28. Tosoni A, Nicolardi L and Brandes AA: Current clinical management of gastrointestinal stromal tumors. Expert Rev Anticancer Ther 4: 595-605, 2004.
29. Ruka W, Rutkowski P, Nowecki Z, Nasierowska-Guttmejer A and Debiec-Rychter M: Other malignant neoplasms in patients with gastrointestinal stromal tumors (GIST). Med Sci Monit 10: LE13-LE14, 2004.
30. Rutkowski P, Nowecki ZI, Michej W, Debiec-Rychter M, Woźniak A, Limon J, Siedlecki J, Grzesiakowska U, Kakol M, Osuch C, *et al*: Risk criteria and prognostic factors for predicting recurrences after resection of primary gastrointestinal stromal tumor. Ann Surg Oncol 14: 2018-2027, 2007.
31. Hirota S, Isozaki K, Moriyama Y, Hashimoto K, Nishida T, Ishiguro S, Kawano K, Hanada M, Kurata A, Takeda M, *et al*: Gain-of-function mutations of c-kit in human gastrointestinal stromal tumors. Science 279: 577-580, 1998.
32. Chompret A, Kannengiesser C, Barrois M, Terrier P, Dahan P, Tursz T, Lenoir GM and Bressac-De Paillerets B: PDGFRA germline mutation in a family with multiple cases of gastrointestinal stromal tumor. Gastroenterology 126: 318-321, 2004.
33. Kwon JE, Kang HJ, Kim SH, Lee YC, Hyung WJ, Noh SH, Kim NK and Kim H: Pathological characteristics of gastrointestinal stromal tumours with PDGFRA mutations. Pathology 41: 544-554, 2009.
34. Schaefer IM, Ströbel P, Cameron S, Beham A, Otto C, Schildhaus HU and Agaimy A: Rhabdoid morphology in gastrointestinal stromal tumours (GISTs) is associated with PDGFRA mutations but does not imply aggressive behaviour. Histopathology 64: 421-430, 2014.
35. Gunawan B, Bergmann F, Höer J, Langer C, Schumpelick V, Becker H and Füzesi L: Biological and clinical significance of cytogenetic abnormalities in low-risk and high-risk gastrointestinal stromal tumors. Hum Pathol 33: 316-321, 2002.
36. Schoppmann SF, Vinatzer U, Popitsch N, Mittlböck M, Liebmann-Reindl S, Jomrich G, Streubel B and Birner P: Novel clinically relevant genes in gastrointestinal stromal tumors identified by exome sequencing. Clin Cancer Res 19: 5329-5339, 2013.
37. Wozniak A, Sciot R, Guillou L, Pauwels P, Wasag B, Stul M, Vermeesch JR, Vandenberghe P, Limon J and Debiec-Rychter M: Array CGH analysis in primary gastrointestinal stromal tumors: Cytogenetic profile correlates with anatomic site and tumor aggressiveness, irrespective of mutational status. Genes Chromosomes Cancer 46: 261-276, 2007.
38. Astolfi A, Nannini M, Pantaleo MA, Di Battista M, Heinrich MC, Santini D, Catena F, Corless CL, Maleddu A, Saponara M, *et al*: A molecular portrait of gastrointestinal stromal tumors: An integrative analysis of gene expression profiling and high-resolution genomic copy number. Lab Invest 90: 1285-1294, 2010.
39. Lagarde P, Pérot G, Kauffmann A, Brulard C, Dapremont V, Hostein I, Neuville A, Wozniak A, Sciot R, Schöffski P, *et al*: Mitotic checkpoints and chromosome instability are strong predictors of clinical outcome in gastrointestinal stromal tumors. Clin Cancer Res 18: 826-838, 2012.
40. Liu CH, Chen TC, Chau GY, Jan YH, Chen CH, Hsu CN, Lin KT, Juang YL, Lu PJ, Cheng HC, *et al*: Analysis of protein-protein interactions in cross-talk pathways reveals CRKL protein as a novel prognostic marker in hepatocellular carcinoma. Mol Cell Proteomics 12: 1335-1349, 2013.